Neutrino-induced single-pion production: from threshold to high invariant masses

Raúl González Jiménez

Department of Physics and Astronomy, Ghent University, Belgium

2017 International Summer School on Reaction Theory
June 12-22, 2017 @ Bloomington, Indiana, US

20 June 2017

In collaboration with...

Ghent

Natalie Jachowicz

Jannes Nys

Vishvas Pandey

Tom Van Cuyck

Nils Van Dessel

Ghent + Wroclaw

Kajetan Niewczas

Electroweak single-pion production off the nucleon: from threshold to high invariant masses

R. González-Jiménez,[1,*] N. Jachowicz,[1] K. Niewczas,[1,2]
J. Nys,[1] V. Pandey,[3] T. Van Cuyck,[1] and N. Van Dessel[1]

[1]*Department of Physics and Astronomy,*
Ghent University, Proeftuinstraat 86,
B-9000 Gent, Belgium
[2]*Institute of Theoretical Physics,*
University of Wrocław, pl. M. Borna 9,
50-204 Wrocław, Poland
[3]*Center for Neutrino Physics, Virginia Tech,*
Blacksburg, Virginia 24061, USA
(Dated: May 11, 2017)

Reference: arXiv:1612.05511v2, soon in Phys. Rev. D

Neutrino oscillations

To determine the **neutrino oscillation** parameters we need to know the energy of the neutrino:

$$P(\nu_x \to \nu_y) = \sin^2 2\theta \sin^2\left(1.27\frac{\Delta m^2(eV^2)L(km)}{E(GeV)}\right)$$

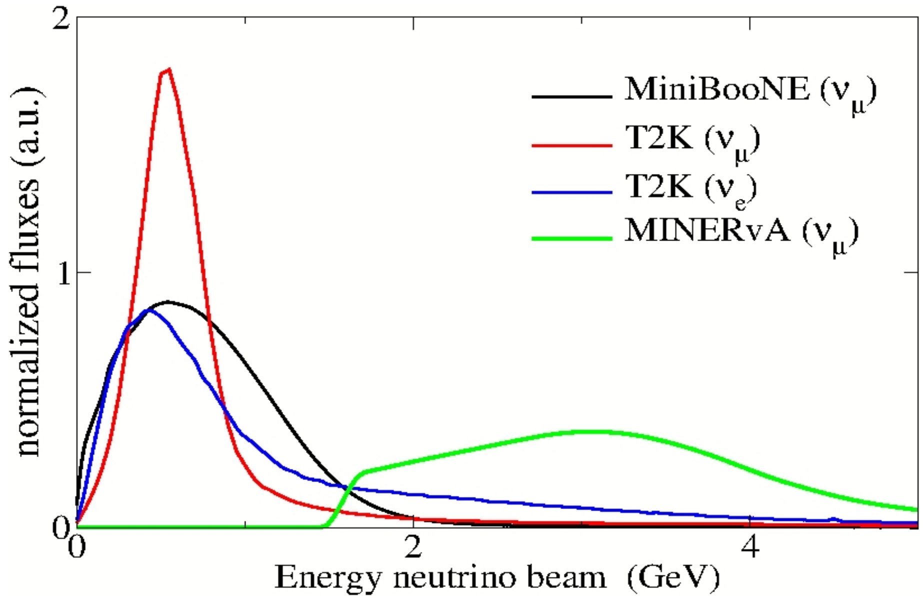

The energy of the neutrino beam is known.
It is **reconstructed** from theoretical information (cross sections) and experimental data.

The **main source of systematic uncertainties** in neutrino oscillation analyses is related with the poor knowledge of the neutrino-nucleus cross sections.

Electroweak single-pion production

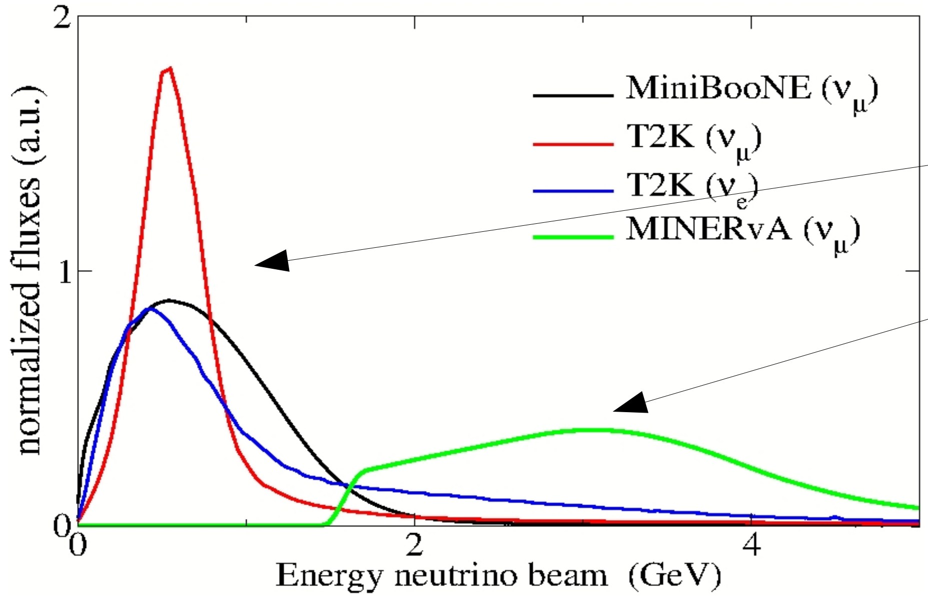

Experiments are shifting the neutrino beam to higher energies: **Single-pion production becomes dominant.**

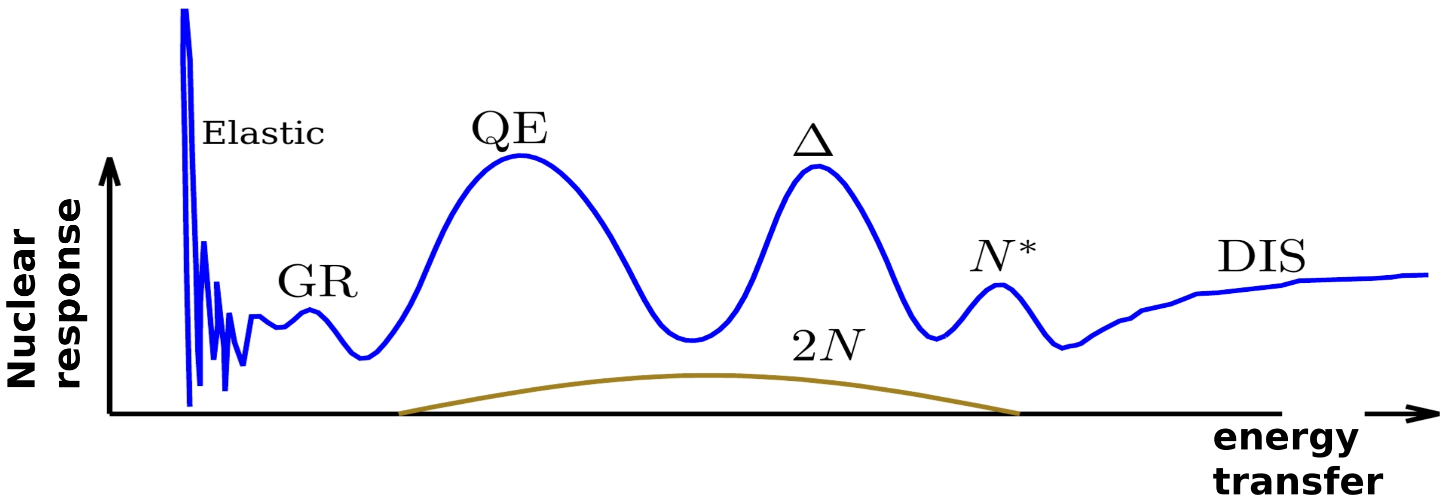

Electroweak single-pion production

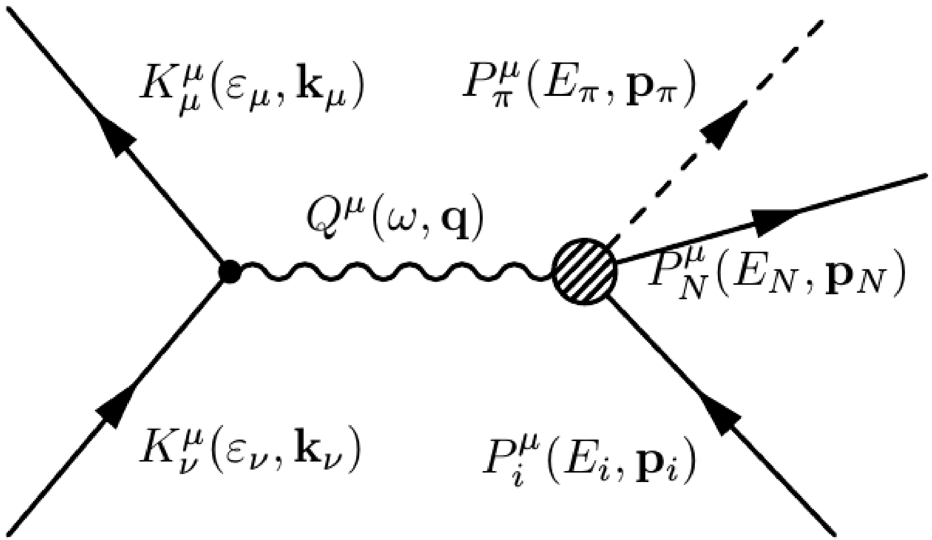

We want a model to make predictions

+ in the resonance region W < 2 GeV and ,

+ in the high-energy energy region W > 2 GeV

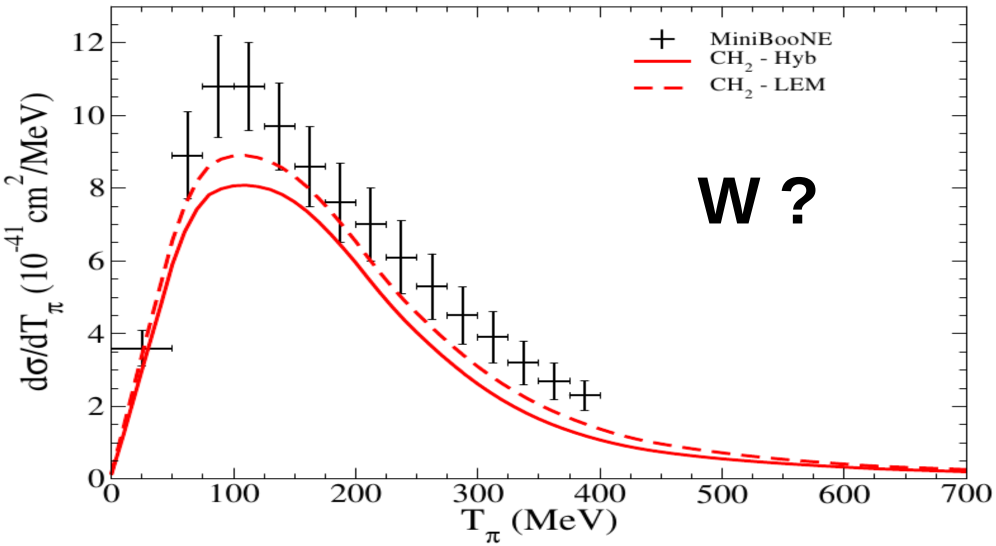

Low-energy model

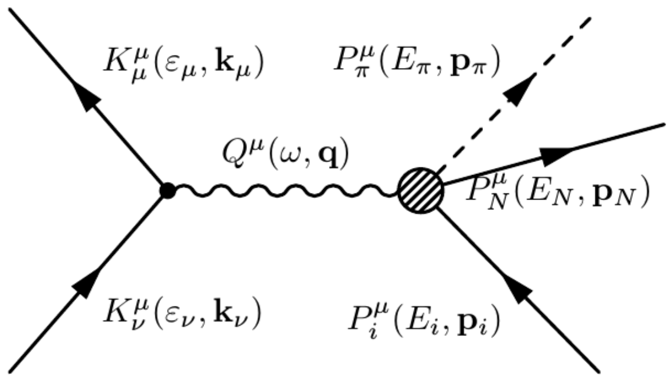

Low-energy model for pion-production on the nucleon:
ChPT background + Resonances
(PRD 76 (2007) 033005, PRD 87 (2013) 113009)

Resonances:
P33(1232), D13(1520), S11(1535), P11(1440)

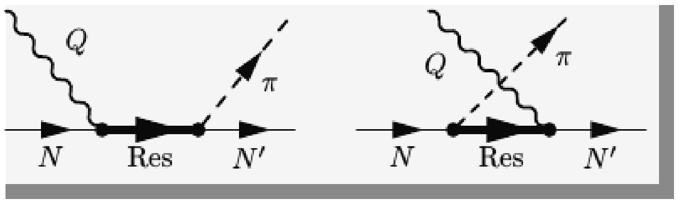

ChPT background:

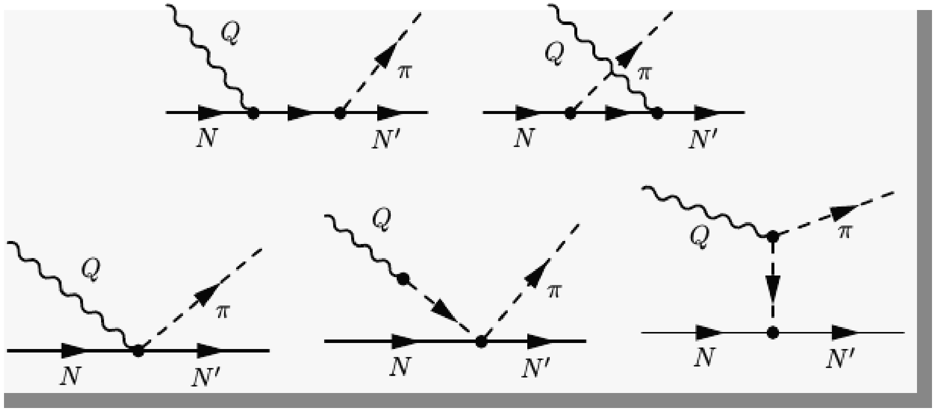

The Problem

Low-energy model
(resonances + ChPT bg)

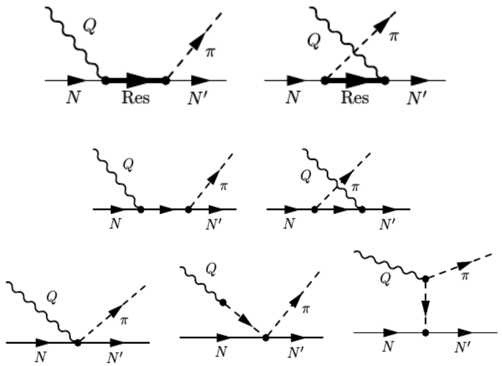

Unphysical predictions at large invariant masses.

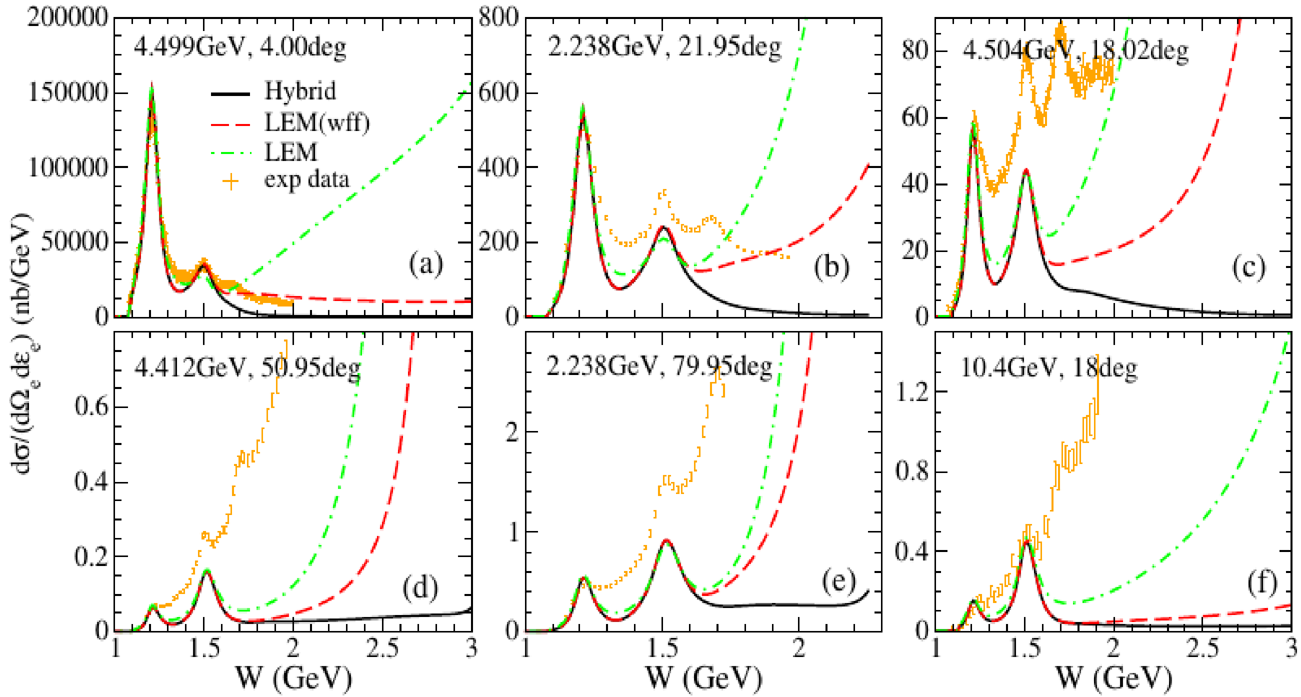

Figure: The model overshoots **inclusive electron-proton** scattering data.

The Problem

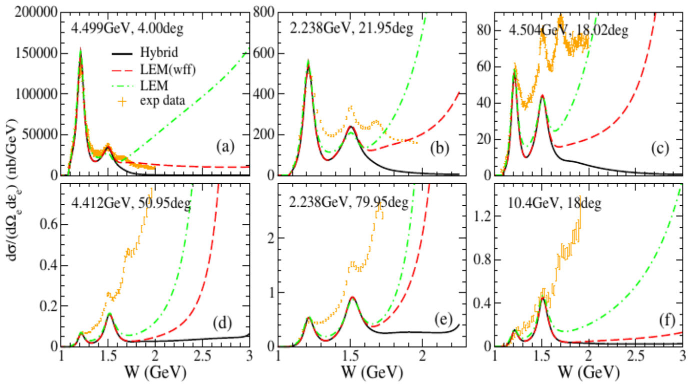

The pathologies come from the

resonances and **background terms**

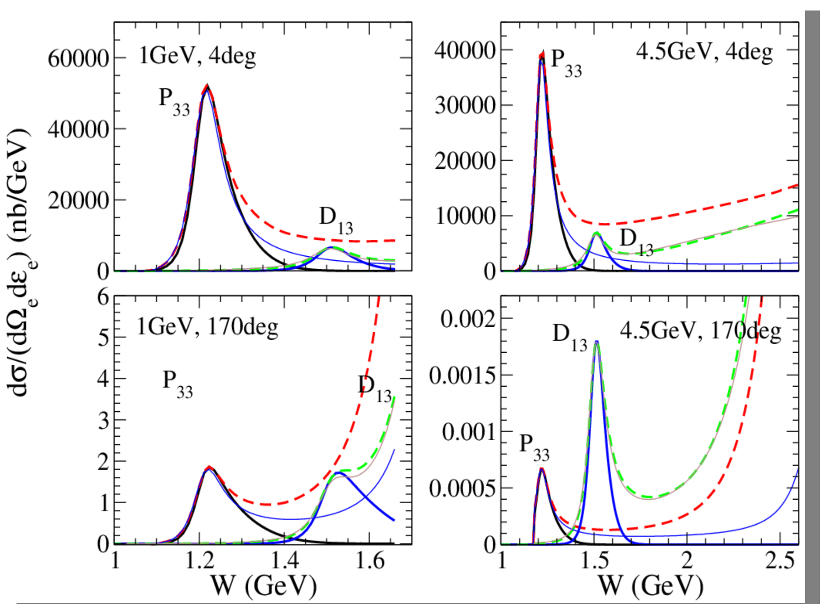

Electron scattering

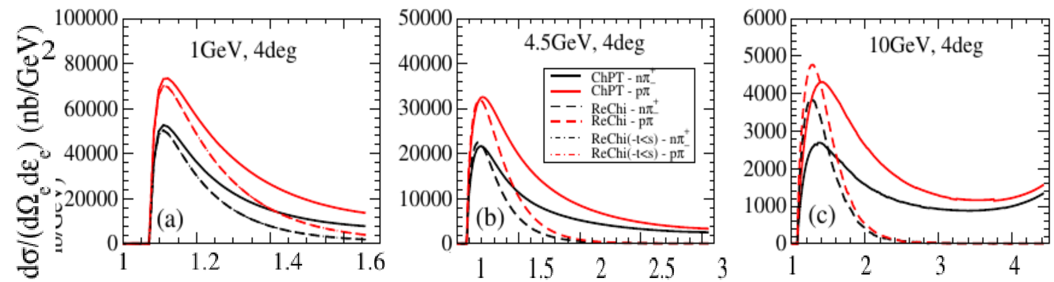

WNC neutrino scattering

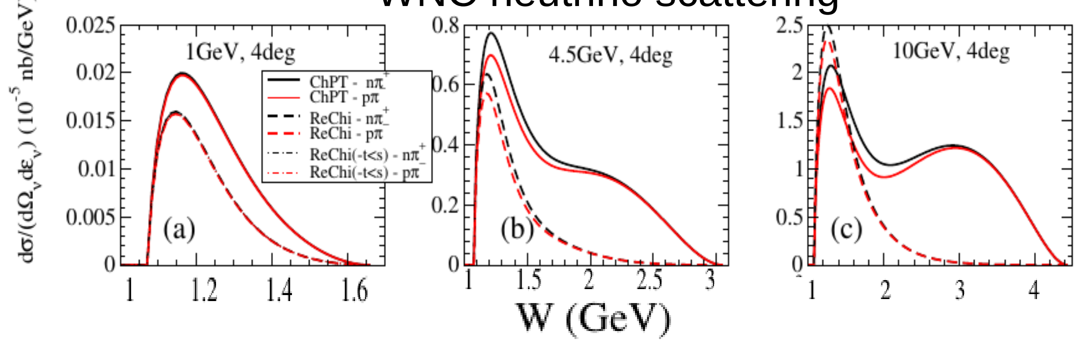

Why does this happen?

Cross channels: 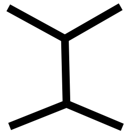

$$\mathcal{A}(t,s) = \sum_{\ell} (2\ell+1)\, A_\ell(t)\, P_\ell(z_t)$$

$$z_t \equiv \cos\theta_t = 1 + \frac{2s}{t-4m^2}$$

$$P_\ell(z_t) \xrightarrow{s\to\infty} (2s)^\ell$$

Direct channels: 

$$\mathcal{A}(s,t) = \sum_{\ell} (2\ell+1)\, A_\ell(s)\, P_\ell(z_s)$$

$$z_s \equiv \cos\theta_s = 1 + \frac{2t}{s-4m^2}$$

$$A_\ell(s) \sim \left(\frac{s-4m^2}{2}\right)^\ell$$

Behavior at threshold (barrier factor).
Feynman diagrams provide the right behavior at threshold but not at high s

High-energy model

Reggeizing the hadronic vector-current operator.

We use the approach of Guidal, Laget, and Vanderhaeghen [NPA627, 645 (1997)], originally developed for pion photoproduction ($Q^2 = 0$):

1) Feynman meson-exchange diagrams are reggeized
2) s-channel and u-channel diagrams are included to keep CVC.

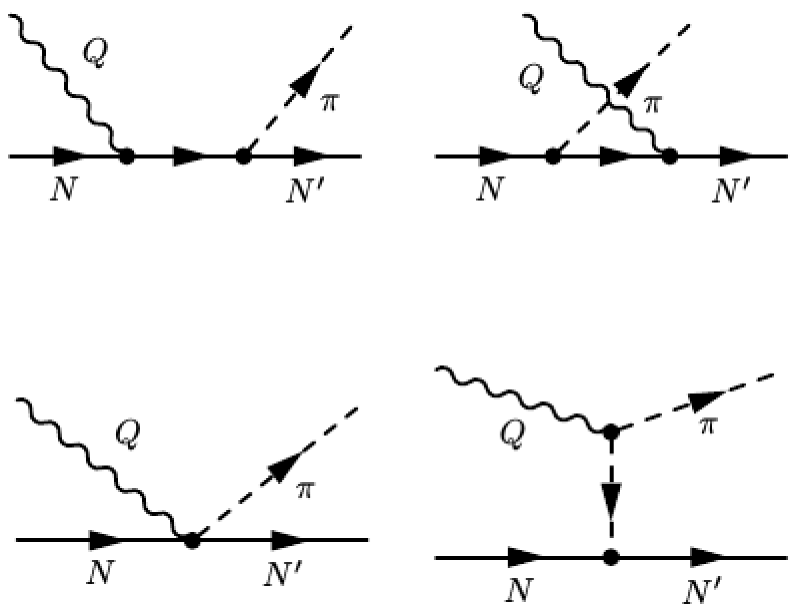

High-energy model

Reggeizing the hadronic vector-current operator.

We use the approach of Guidal, Laget, and Vanderhaeghen [NPA627, 645 (1997)], originally developed for pion photoproduction ($Q^2 = 0$):

1) Feynman **meson-exchange diagrams** are reggeized

2) s-channel and u-channel diagrams are included to keep **Conservation of Vector Current** (gauge invariance).

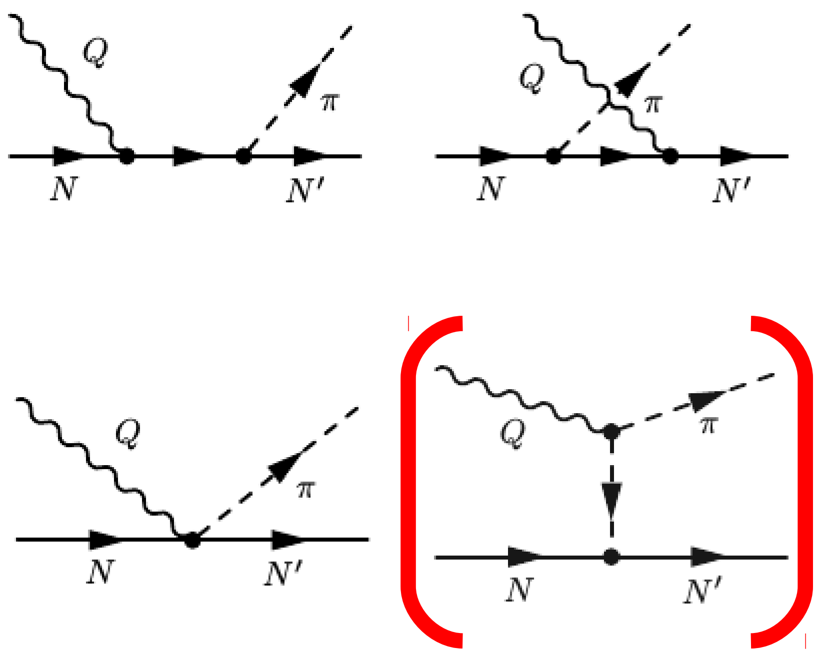

$$\frac{1}{t - m_\pi^2}$$

The pion propagator is replace by the Regge trajectory of the pion family

$$\mathcal{P}_\pi(t,s) = -\alpha'_\pi \varphi_\pi(t)\Gamma[-\alpha_\pi(t)](\alpha'_\pi s)^{\alpha_\pi(t)}$$

High-energy model

Reggeizing the hadronic vector-current operator.

We use the approach first proposed by Kaskulov and Mosel [PRC81, 045202 (2010)] to extends GLV to the case of pion electroproduction ($Q^2 \neq 0$).

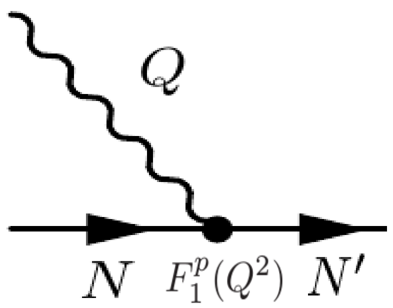

The nucleon N' may be highly off its mass shell.
Therefore, insteed of using the on shell form factor $F_1^p(Q^2)$.
we use a form factor that accounts for the off shell character of the nucleon [Vrancx and Ryckebusch, PRC89, 025203 (2014)]:

$$F_1^p(Q^2, s) = \left(1 + \frac{Q^2}{\Lambda_{\gamma pp^*}(s)^2}\right)^{-2}$$

$$\Lambda_{\gamma pp^*}(s) = \Lambda_{\gamma pp} + (\Lambda_\infty - \Lambda_{\gamma pp})\left(1 - \frac{M^2}{s}\right)$$

$$\Lambda_\infty = 2.194 \text{ GeV}$$

In the (on shell) limit the Dirac form factor is recovered.

High-energy model: results (EM current)

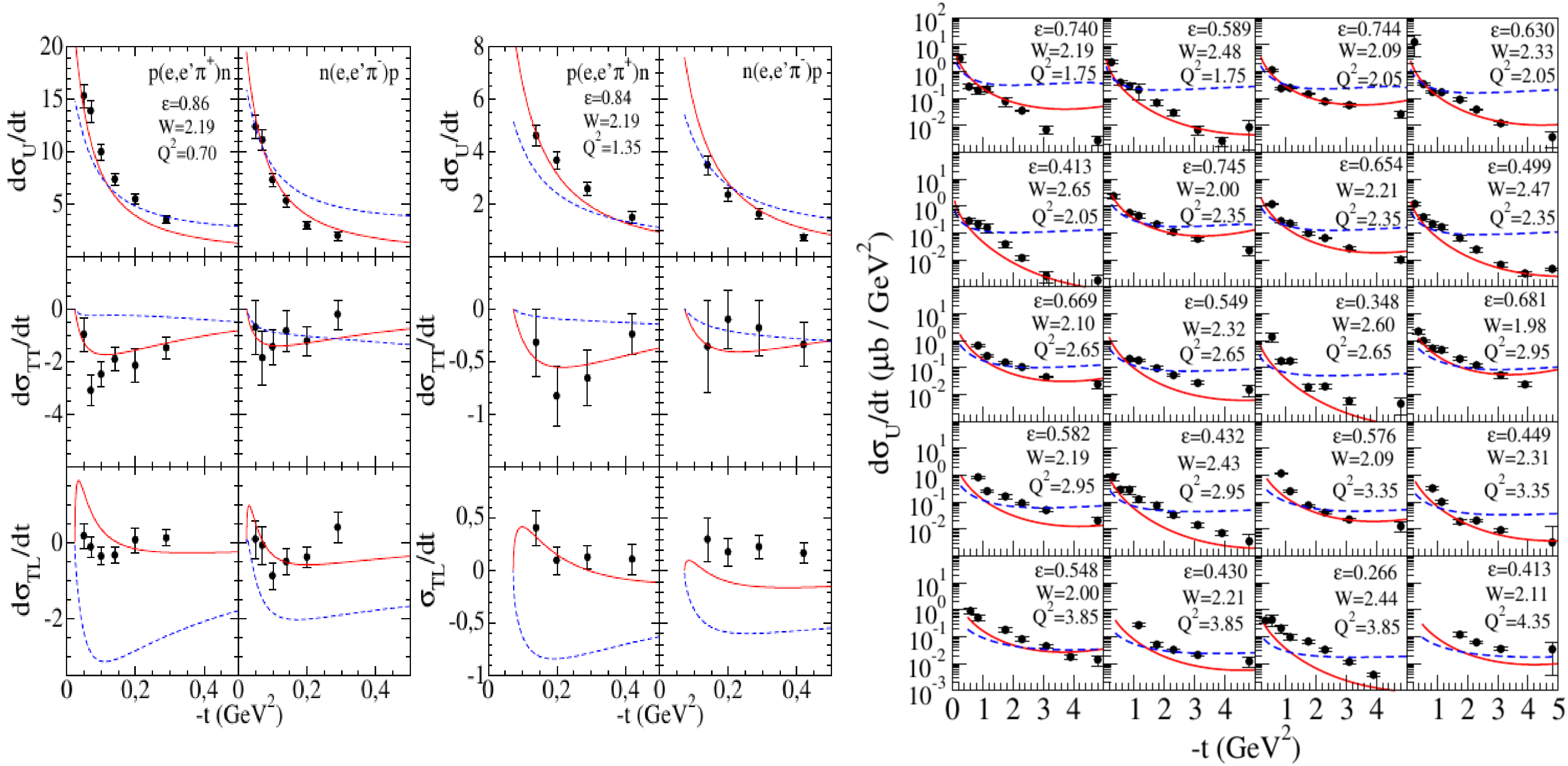

Figure: High-energy model (red lines), low-energy model (blue lines) and **electron-induced single-pion production** data.

High-energy model

Reggeizing the hadronic axial current operator:

We need meson exchange diagrams to apply the reggeization procedure of the current.

Effective rho-exchange diagrams. This allows us to consider the rho-exchange as the main Regge trajectory in the axial current.

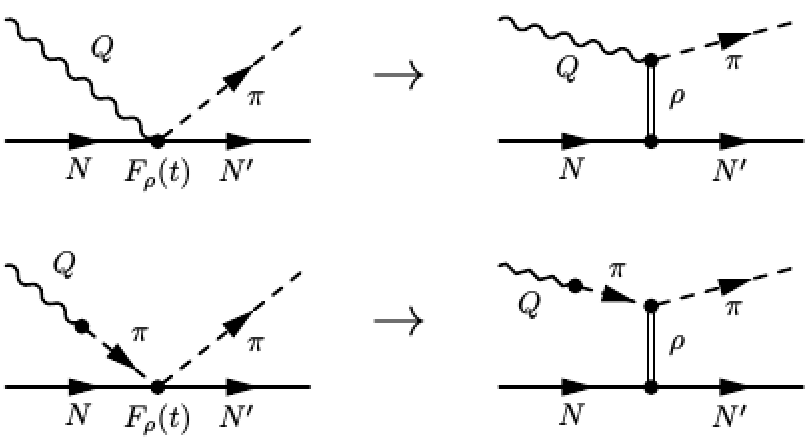

$$\mathcal{O}^{\mu}_{CT\rho} = i\mathcal{I}\,\frac{m_\rho^2}{m_\rho^2 - t}F_{A\rho\pi}(Q^2)\frac{1}{\sqrt{2}f_\pi} \times \left(\gamma^\mu + i\frac{\kappa_\rho}{2M}\sigma^{\mu\nu}K_{t,\nu}\right).$$

We consider $\kappa_\rho = 0$ so that the low-energy model amplitude is recovered.

The propagator of the rho is replaced by the Regge trajectory of the rho family:

$$\mathcal{P}_\rho(t,s) = -\alpha'_\rho \varphi_\rho(t)\Gamma[1-\alpha_\rho(t)](\alpha'_\rho s)^{\alpha_\rho(t)-1}$$

High-energy model

Reggeizing the hadronic axial current operator:

We need meson exchange diagrams to apply the reggeization procedure of the current.

Effective rho-exchange diagrams. This allows us to consider the rho-exchange as the main Regge trajectory in the axial current.

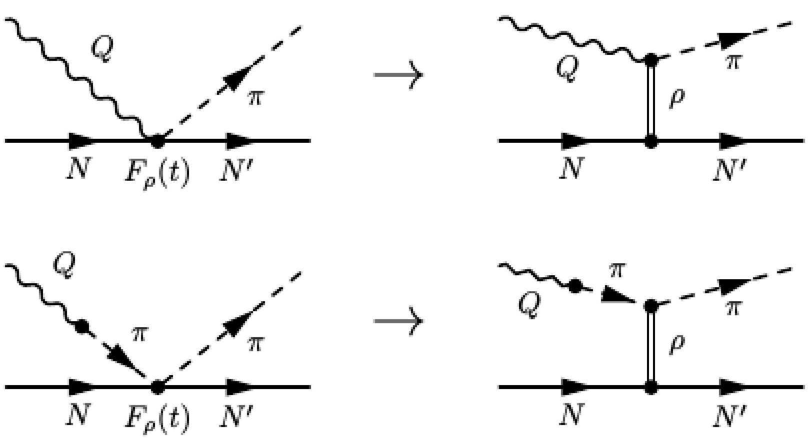

$$\mathcal{O}^{\mu}_{CT\rho} = i\mathcal{I}\,\frac{m_\rho^2}{m_\rho^2 - t} F_{A\rho\pi}(Q^2)\,\frac{1}{\sqrt{2}f_\pi} \times \left(\gamma^\mu + i\frac{\kappa_\rho}{2M}\sigma^{\mu\nu}K_{t,\nu}\right).$$

We consider $\kappa_\rho = 0$ so that the low-energy model amplitude is recovered.

+ 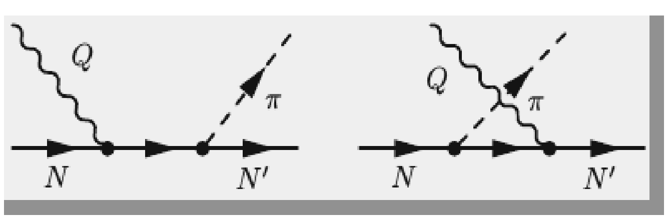

?

High-energy model

Reggeizing the hadronic the ChPT background:

$$\mathcal{O}^{\mu}_{ReChi,V} = \mathcal{O}^{\mu}_{ChPT,V}\, \underbrace{\mathcal{P}_{\pi}(t,s)(t-m_{\pi}^{2})}$$

high-energy model: ReChi (from Reggeized ChPT background)

low-energy model (only the ChPT background)

The pion propagator is replaced by the **Regge propagator** of the pion trajectory

$$\mathcal{O}^{\mu}_{ReChi,A} = \mathcal{O}^{\mu}_{ChPT,A}\, \mathcal{P}_{\rho}(t,s)(t-m_{\rho}^{2})$$

High-energy model: results

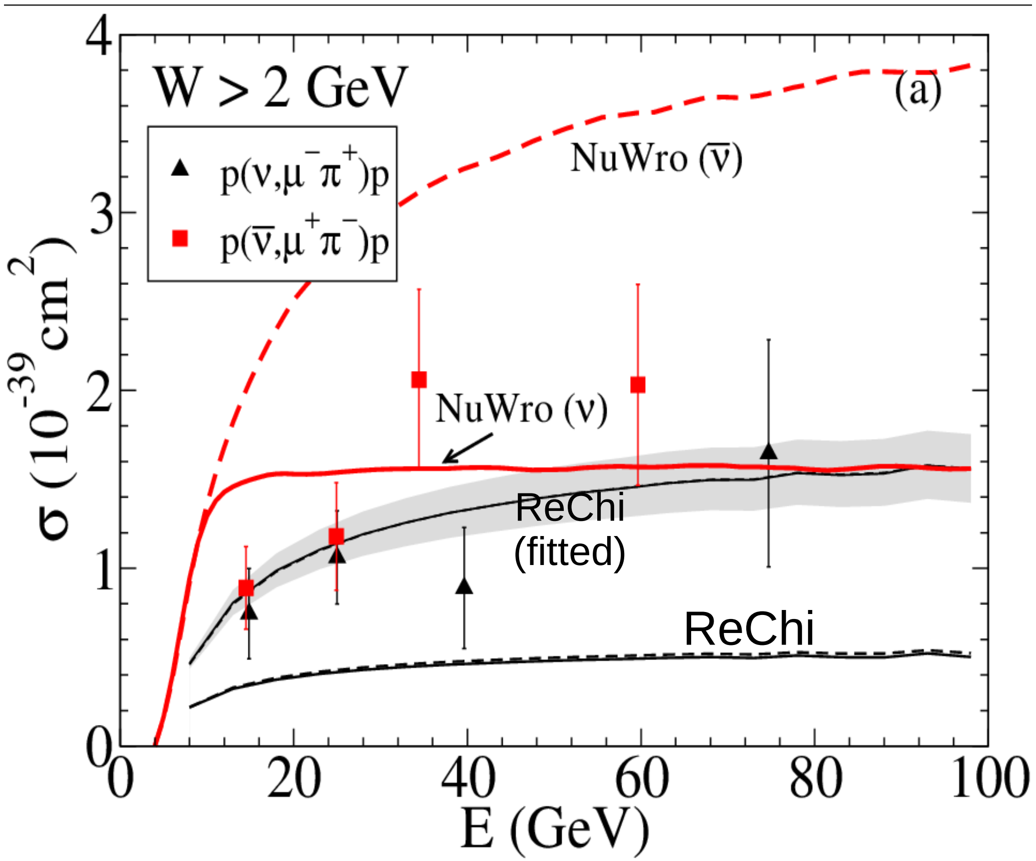

Figure: ReChi model and NuWro predictions are compared with high energy cross section data for neutrino and antineutrino reactions (Note the high energy cut W>2 GeV !!). Data from Allen et al. NPB264, 221 (1986).

ReChi model: One free parameter in the boson-nucleon-nucleon vertex

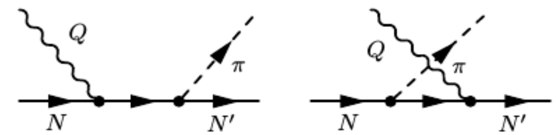

$$G_A[Q^2, s(u)] = g_A \left(1 + \frac{Q^2}{\Lambda_{Apn^*}[s(u)]^2}\right)^{-2}$$

$$\Lambda_{Anp^*}(s) = \Lambda_{Apn} + (\Lambda_\infty^A - \Lambda_{Apn})\left(1 - \frac{M^2}{s}\right)$$

$$\Lambda_\infty^A = (7.20 \pm {}^{2.09}_{1.32})\ \mathrm{GeV}$$!!!

NuWro: Based on DIS formalism and PYTHIA for hadronization.

Antineutrino cross section is ~2 the neutrino one:

$$\bar{\nu} + \overbrace{uud}^{p} \rightarrow \mu^+ + \overbrace{\bar{u}d}^{\pi^-} + uud\,,$$

$$\nu + uud \rightarrow \mu^- + \underbrace{u\bar{d}}_{\pi^+} + uud\,.$$

Hybrid model

1) Regularizing the behavior of resonances (u- and s-channel contributions): we multiply the resonance amplitude by a dipole-Gaussian form factor

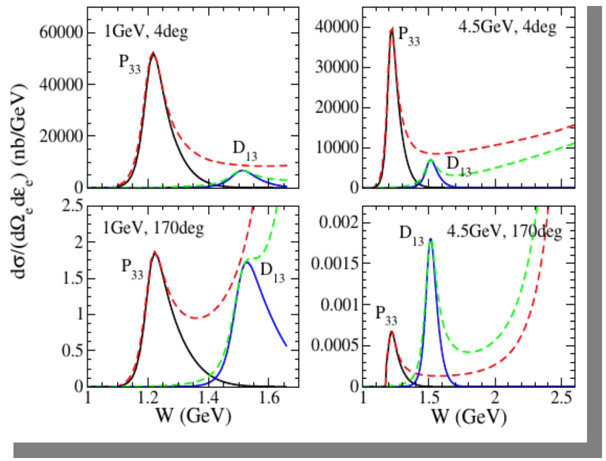

$$F(s,u) = F(s) + F(u) - F(s)F(u)$$

$$F(s) = \exp\left(\frac{-(s-M_R^2)^2}{\lambda_R^4}\right) \frac{\lambda_R^4}{(s-M_R^2)^2+\lambda_R^4}$$

2) Gradually replacing the ChPT background by the High-energy (ReChi) model: we use a phenomenological transition function

$$\widetilde{\mathcal{O}} = \cos^2\phi(W)\mathcal{O}_{ChPT} + \sin^2\phi(W)\mathcal{O}_{ReChi}$$

$$\phi(W) = \frac{\pi}{2}\left(1 - \frac{1}{1+\exp\left[\frac{W-W_0}{L}\right]}\right) , \quad \begin{aligned} W_0 &= 1.7 \text{ GeV} \\ L &= 100 \text{ MeV} \end{aligned}$$

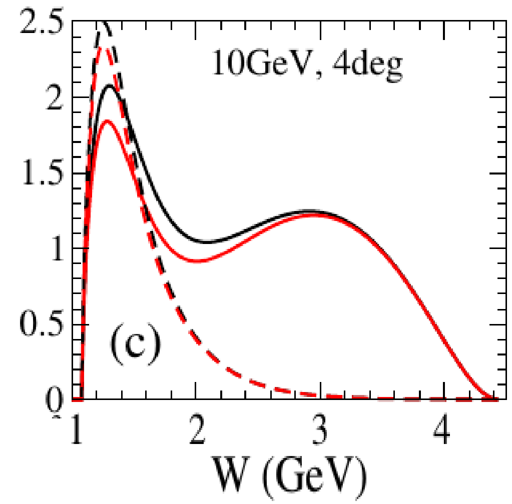

Hybrid model: results

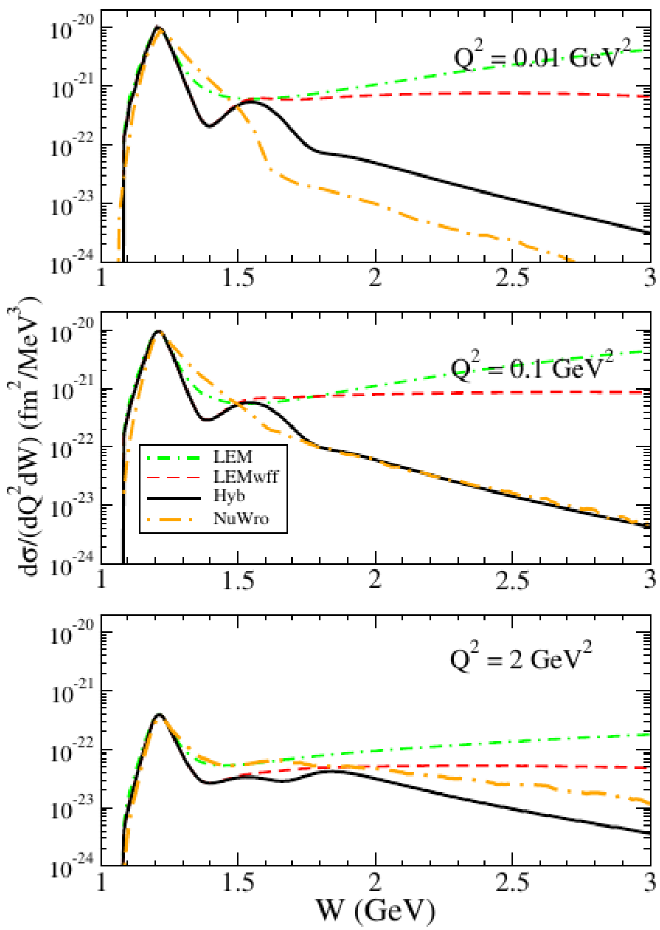

FIG. 21. (Color online) Different model predictions for the differential cross section $d\sigma/(dQ^2dW)$, for the channel $p(\nu_\mu, \mu^-\pi^+)p$. The incoming neutrino energy is fixed to $E_\nu = 10$ GeV.

Hybrid model: results

No cut in W

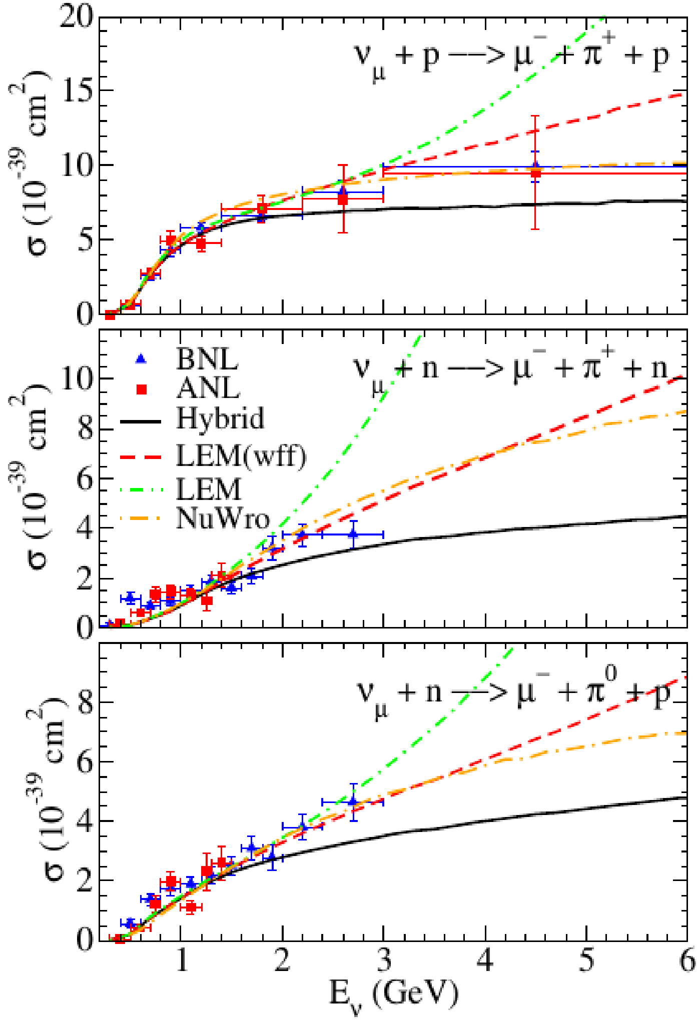

Electroweak one-pion production on nuclei

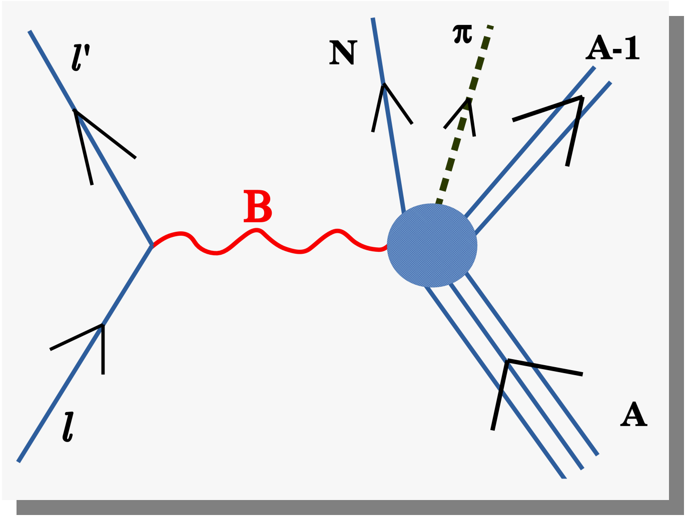

IV. Relativistic mean field model

Relativistic Impulse Approximation

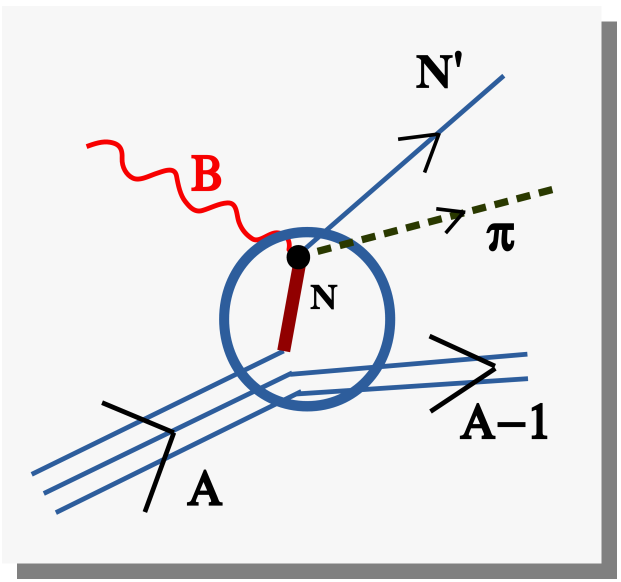

Plane waves (for the moment...)

$$J^{\mu}_{had} = \sum_{i}^{A} \int d\mathbf{r}\, \overline{\Psi}_F(\mathbf{r})\, \phi^*(\mathbf{r}) \hat{O}^{\mu}_{one\text{-}body}(\mathbf{r})\, \Psi_B(\mathbf{r})\, e^{i\mathbf{q}\cdot\mathbf{r}}$$

not yet ?

Relativistic mean-field wave functions

$$[-i\boldsymbol{\alpha}\cdot\boldsymbol{\nabla} + V(r) + \beta(M + S(r)]\Psi_i(\boldsymbol{r}) = E_i\Psi_i(\boldsymbol{r})$$

$$\frac{d^8\sigma}{d\varepsilon_f d\Omega_f dE_\pi d\Omega_\pi d\Omega_N} = \frac{m_i m_f}{(2\pi)^8} \frac{M_N\, p_N\, k_\pi}{E_N\, f_{rec}} \frac{k_f}{\varepsilon_i} \overline{\sum_{fi}} |\mathcal{M}_{fi}|^2$$

8-fold differential cross section: Computationally very demanding

Comparison with MINERvA $\bar{\nu}$ data: $1\pi^0$ sample

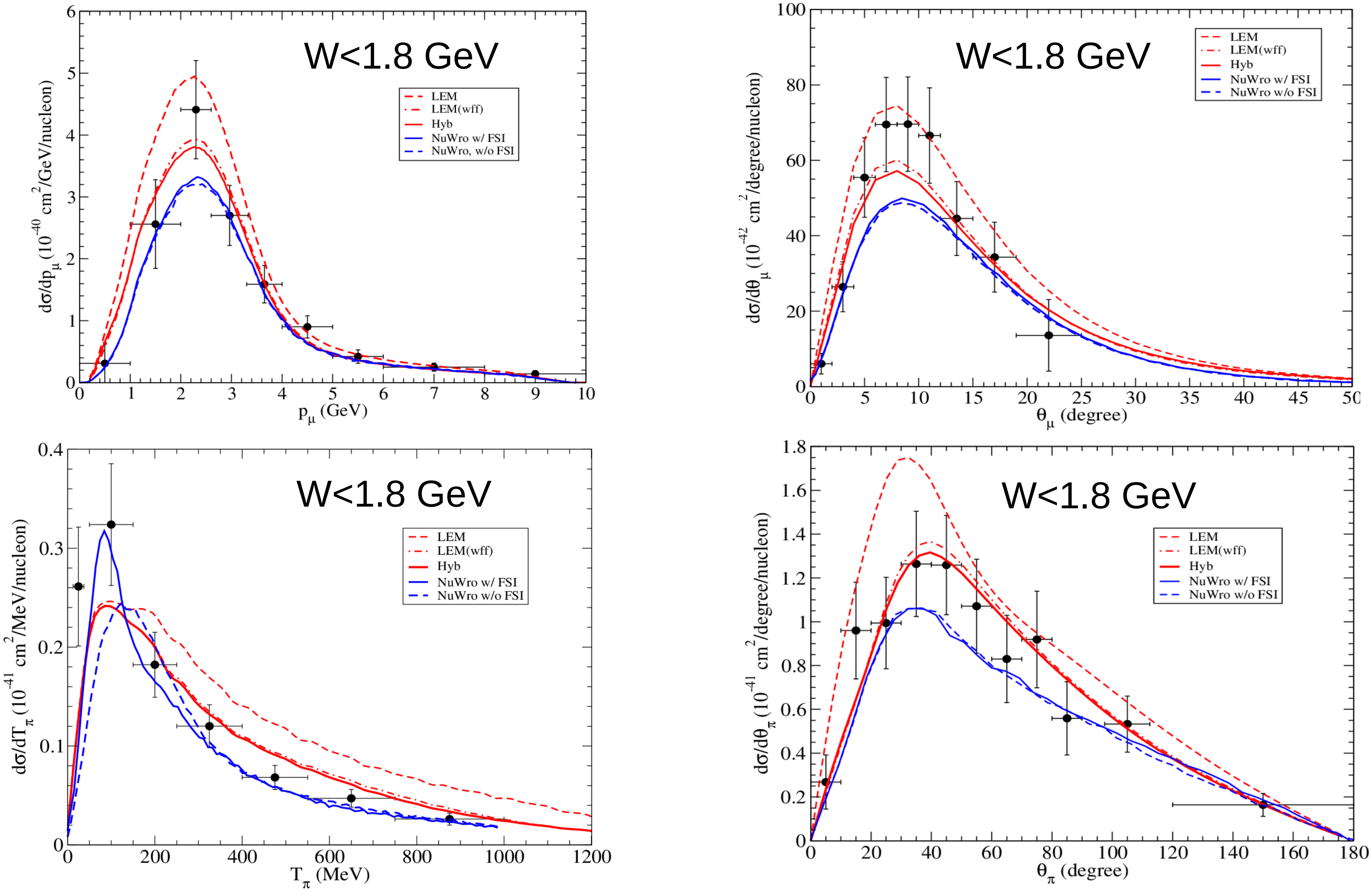

Comparison with MINERvA $\bar{\nu}$ data: $1\pi^0$ sample

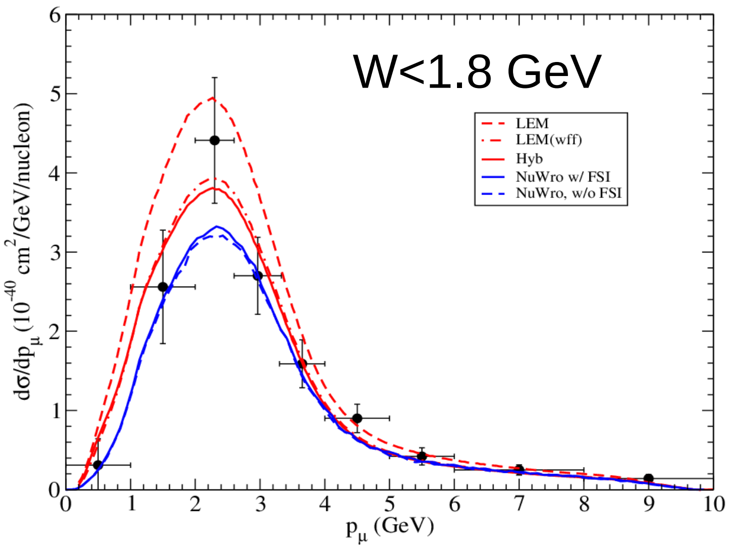

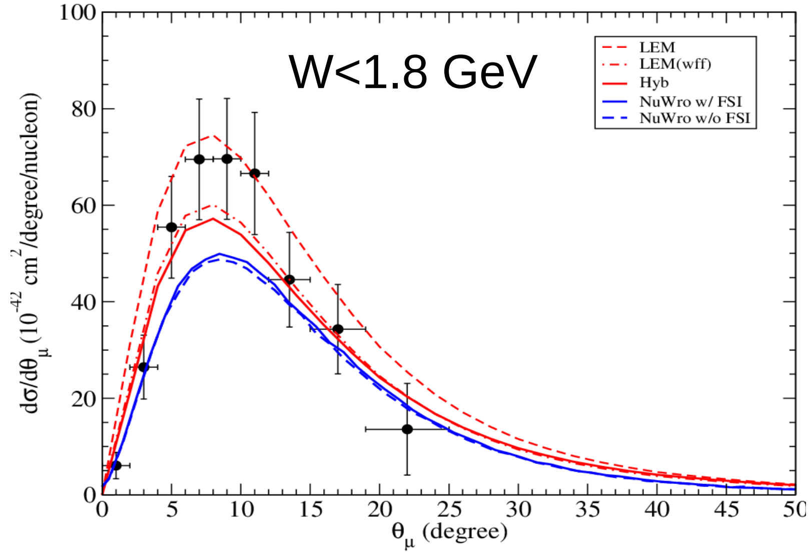

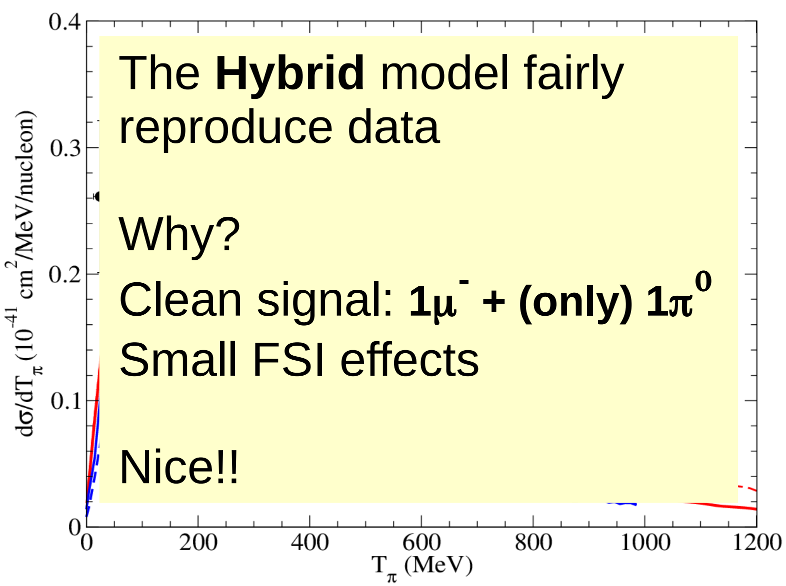

The **Hybrid** model fairly reproduce data

Why?

Clean signal: **$1\mu^-$ + (only) $1\pi^0$**

Small FSI effects

Nice!!

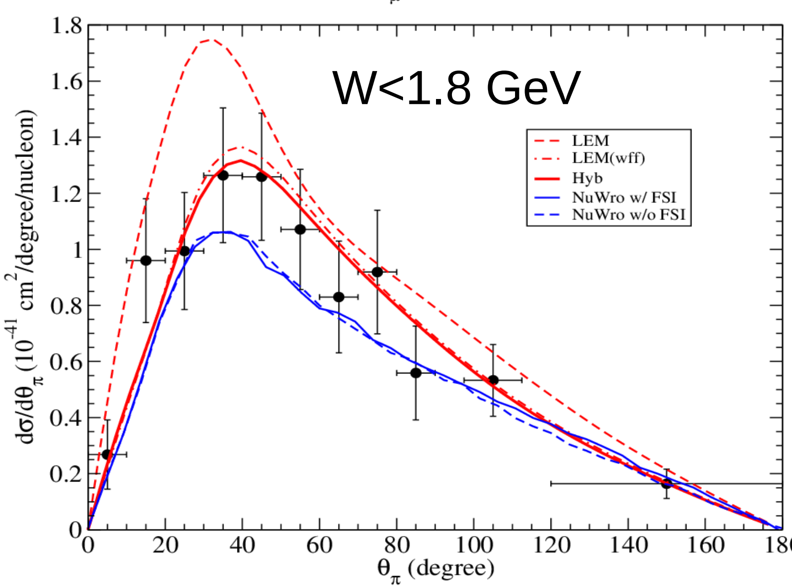

Comparison with MINERvA data: $n\pi^+$ sample

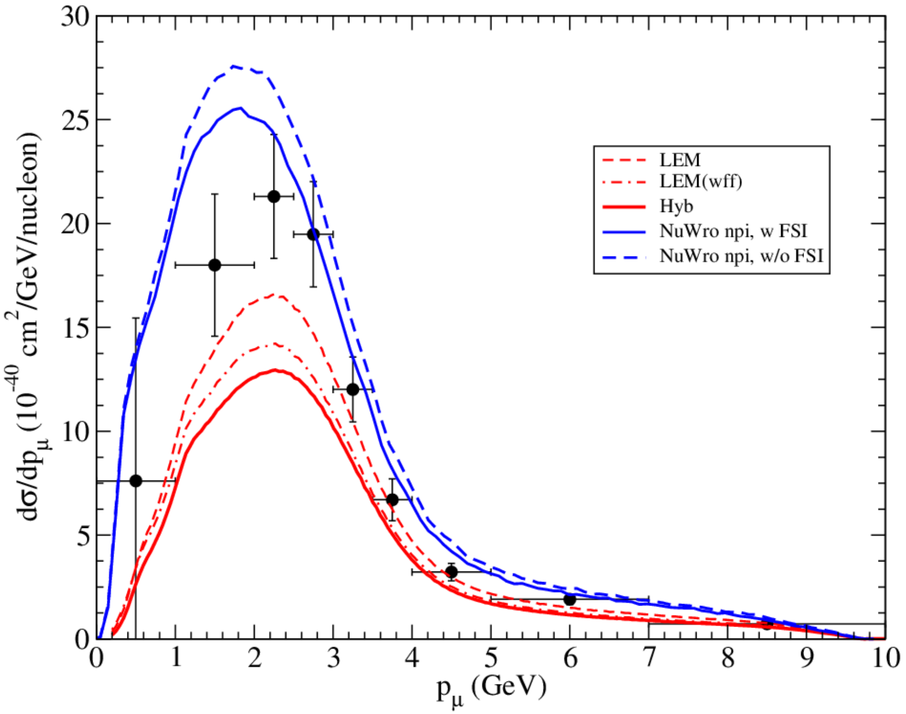

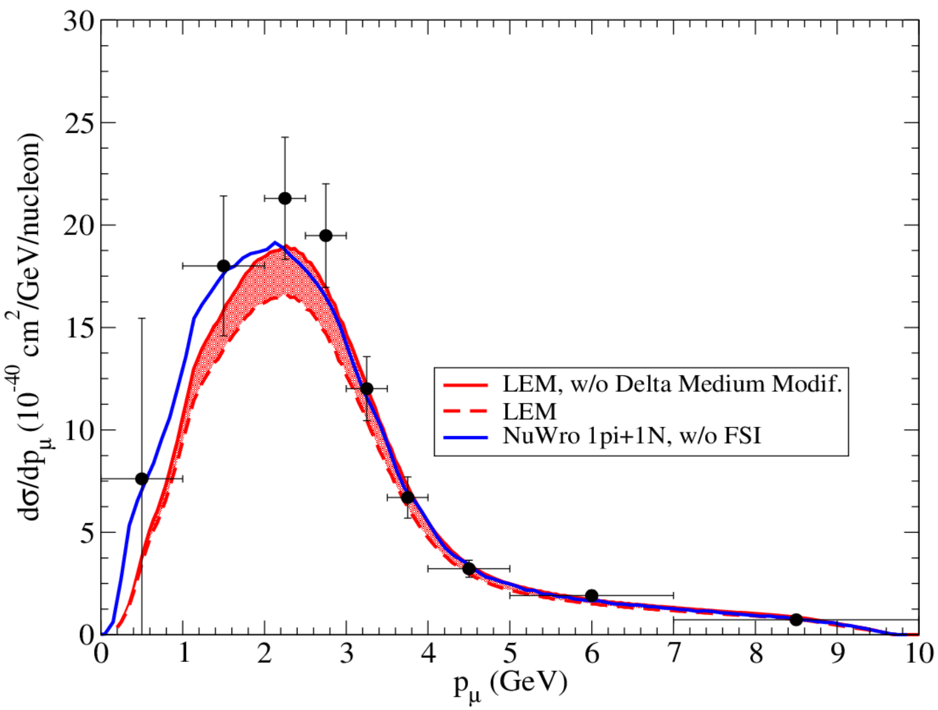

Definition of the Final State (W<1.8 GeV):

Experiment:	$1\mu^- + n\pi^{+/-} + \ldots$
NuWro:	$1\mu^- + n\pi^{+/-} + \ldots$
Our model:	$1\mu^- + 1\pi^+ + 1N$

Definition of the Final State (W<1.8 GeV):

Experiment:	$1\mu^- + n\pi^{+/-} + \ldots$
NuWro (w/o FSI):	$1\mu^- + 1\pi^+ + 1N$
Our model:	$1\mu^- + 1\pi^+ + 1N$

Comparison with total cross section data

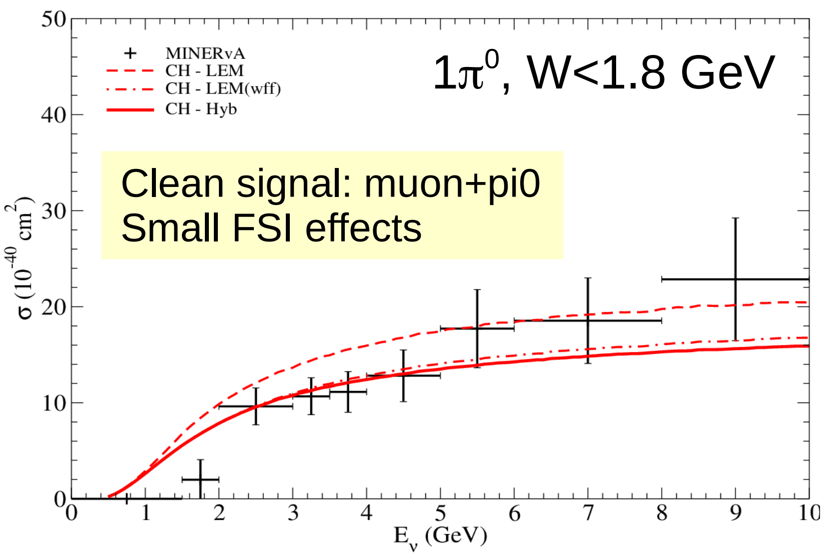

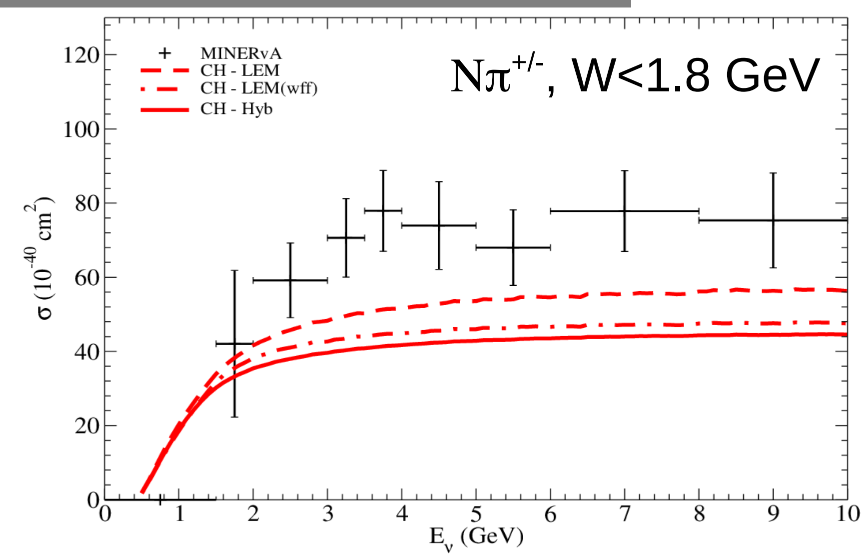

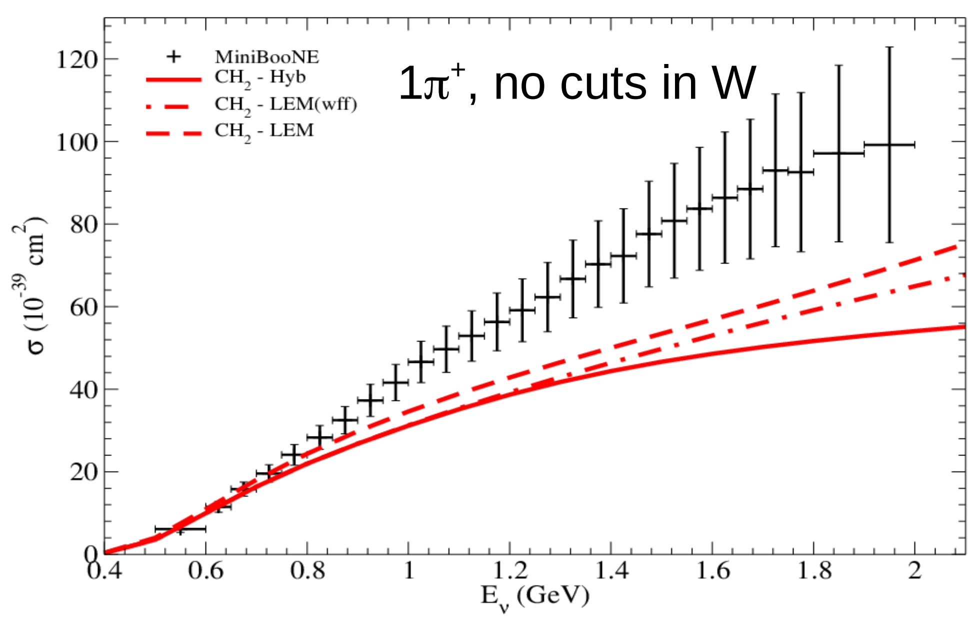

The end...

Thank you

Back slides: more results

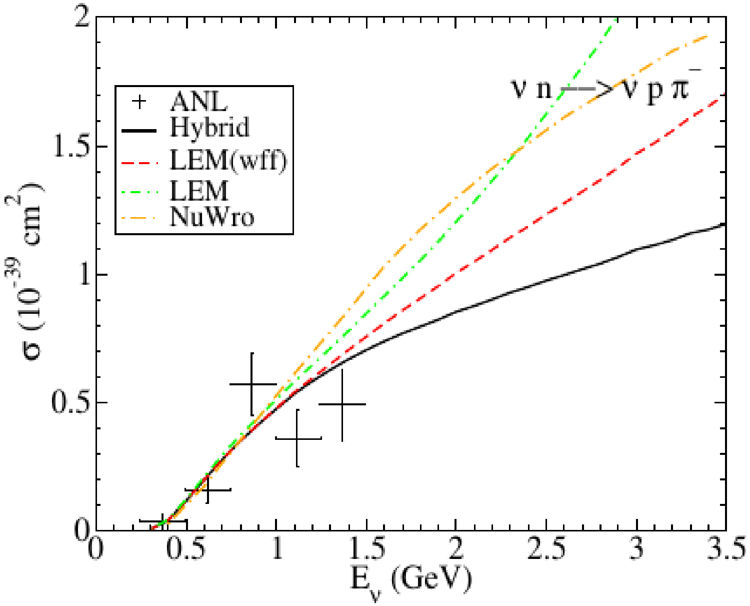

Figure: Predictions for the WNC.

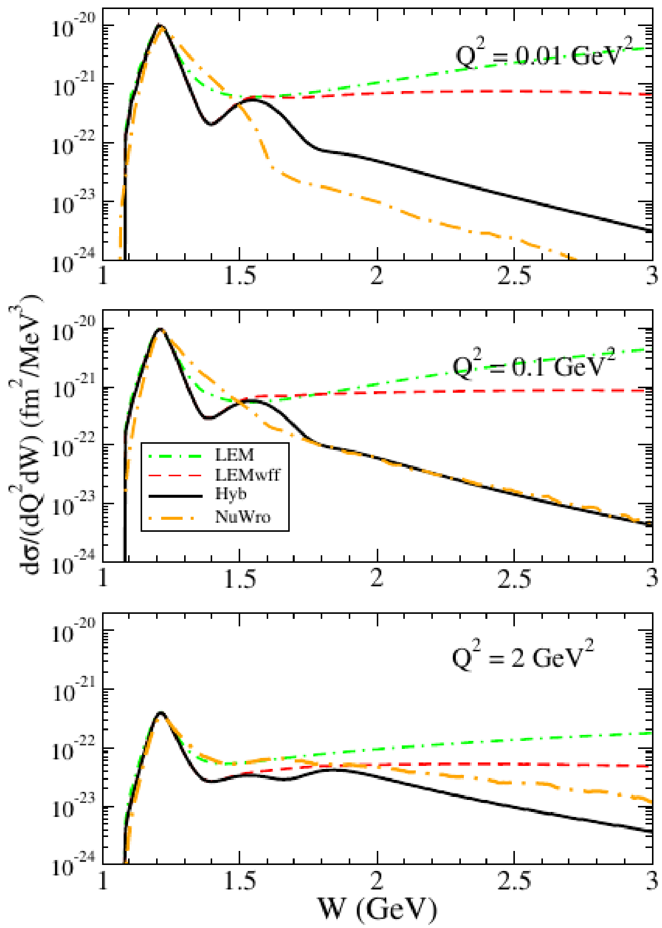

FIG. 21. (Color online) Different model predictions for the differential cross section $d\sigma/(dQ^2dW)$, for the channel $p(\nu_\mu, \mu^- \pi^+)p$. The incoming neutrino energy is fixed to $E_\nu = 10$ GeV.

Back slides: more results

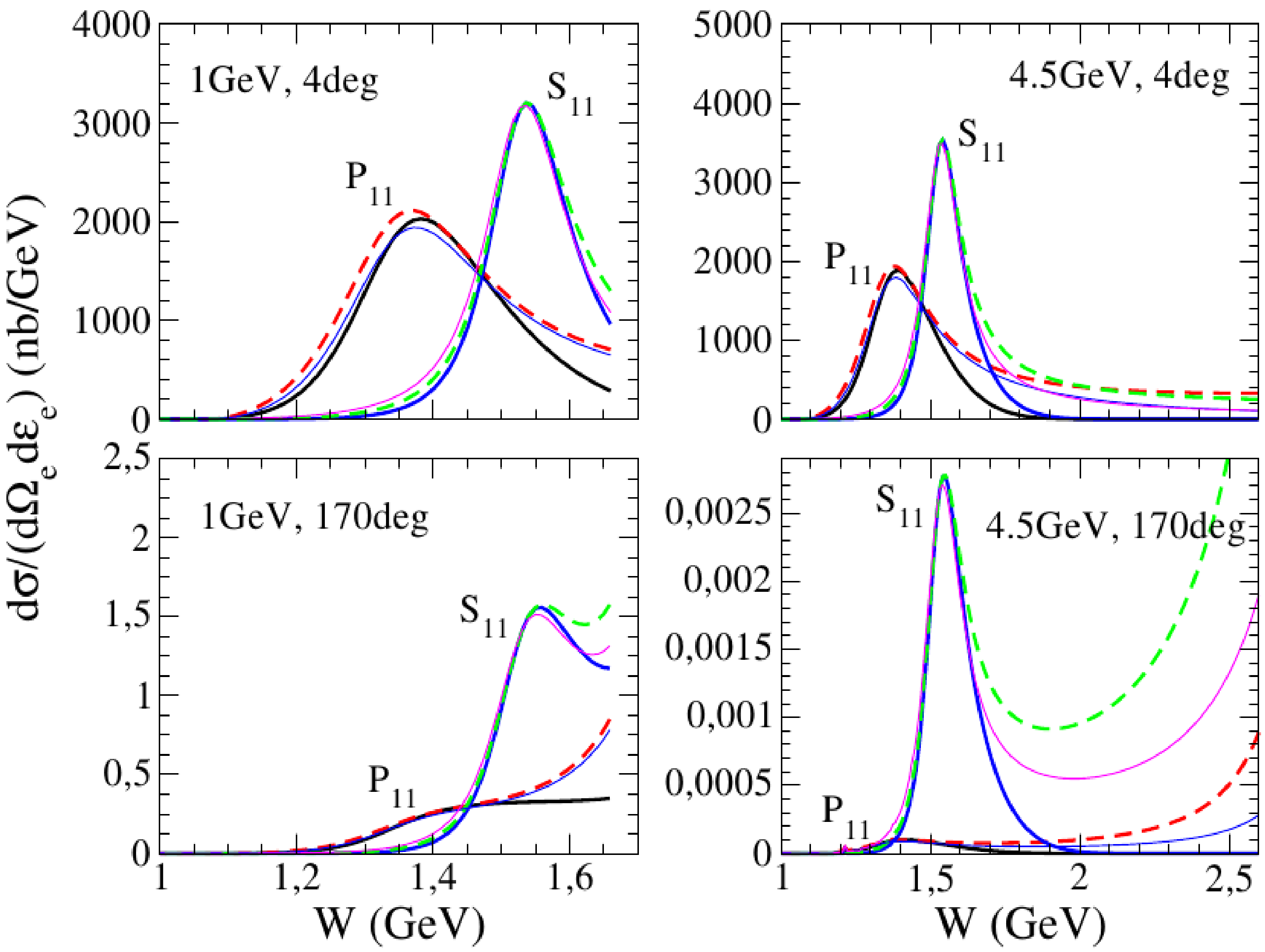

Back slides

$$\mathcal{P}_\pi(t,s) = -\alpha'_\pi \varphi_\pi(t) \Gamma[-\alpha_\pi(t)] (\alpha'_\pi s)^{\alpha_\pi(t)}$$

$$\Gamma[-\alpha_\pi(t)] = -\pi / \{\sin[\pi\alpha_\pi(t)] \Gamma[\alpha_\pi(t)+1]\}$$

The $\Gamma[\alpha_\pi(t)+1]$ removes the unphysical contribution of negative-integer spin exchanges. It is interesting to show that the Regge propagator reduces to the pion propagator near the pion pole

$$\frac{\pi\alpha'_\pi}{\sin[\pi\alpha_\pi(t)]} \underset{t\to m_\pi^2}{\longrightarrow} \frac{1}{t-m_\pi^2} \, . \qquad (35)$$

Back slides: isospin coefficients and resonances parameters

Channel	ΔP	$C\Delta P$	NP	CNP	Others
$p \to \pi^+ + p$	$\sqrt{3/2}$	$\sqrt{1/6}$	0	1	1
$n \to \pi^0 + p$	$-\sqrt{1/3}$	$\sqrt{1/3}$	$\sqrt{1/2}$	$-\sqrt{1/2}$	$-\sqrt{2}$
$n \to \pi^+ + n$	$\sqrt{1/6}$	$\sqrt{3/2}$	1	0	-1
$n \to \pi^- + n$	$\sqrt{3/2}$	$\sqrt{1/6}$	0	1	1
$p \to \pi^0 + n$	$\sqrt{1/3}$	$-\sqrt{1/3}$	$-\sqrt{1/2}$	$\sqrt{1/2}$	$\sqrt{2}$
$p \to \pi^- + p$	$\sqrt{1/6}$	$\sqrt{3/2}$	1	0	-1

Table: Isospin coefficients for the CC reaction.

Channel	ΔP	$C\Delta P$	NP	CNP	Others
$p \to \pi^0 + p$	$\sqrt{1/3}$	$\sqrt{1/3}$	$\sqrt{1/2}$	$\sqrt{1/2}$	0
$p \to \pi^+ + n$	$-\sqrt{1/6}$	$\sqrt{1/6}$	1	1	-1
$n \to \pi^- + p$	$\sqrt{1/6}$	$-\sqrt{1/6}$	1	1	1
$n \to \pi^0 + n$	$\sqrt{1/3}$	$\sqrt{1/3}$	$-\sqrt{1/2}$	$-\sqrt{1/2}$	0

Table: Isospin coefficients for the neutral current (EM and WNC) reactions.

	I	S	P	M_R	πN-br	$\Gamma^{exp}_{\text{width}}$	$f_{\pi NR}$
P_{33}	3/2	3/2	+	1232	100%	120	2.18
D_{13}	1/2	3/2	−	1515	60%	115	1.62
P_{11}	1/2	1/2	+	1430	65%	350	0.391
S_{11}	1/2	1/2	−	1535	45%	150	0.16

Table: quantum numbers and other parameters of the nucleon resonances.

Back slides: Interferences

$$J^\nu = \langle J^\nu_{\Delta P}\rangle + \langle J^\nu_{C\Delta P}\rangle + \langle J^\nu_{CT,V}\rangle + \langle J^\nu_{CT,A}\rangle + \langle J^\nu_{NP}\rangle + \langle J^\nu_{CNP}\rangle + \langle J^\nu_{PF}\rangle + \langle J^\nu_{PP}\rangle$$

PHYSICAL REVIEW D **93,** 014016 (2016)

Watson's theorem and the $N\Delta(1232)$ axial transition

L. Alvarez-Ruso,[1] E. Hernández,[2] J. Nieves,[1] and M. J. Vicente Vacas[3]

We present a new determination of the $N\Delta$ axial form factors from neutrino induced pion production data. For this purpose, the model of Hernandez *et al.* [Phys. Rev. D 76, 033005 (2007)] is improved by partially restoring unitarity. This is accomplished by imposing Watson's theorem on the dominant vector and axial multipoles. As a consequence, a larger $C_5^A(0)$, in good agreement with the prediction from the off-diagonal Goldberger-Treiman relation, is now obtained.

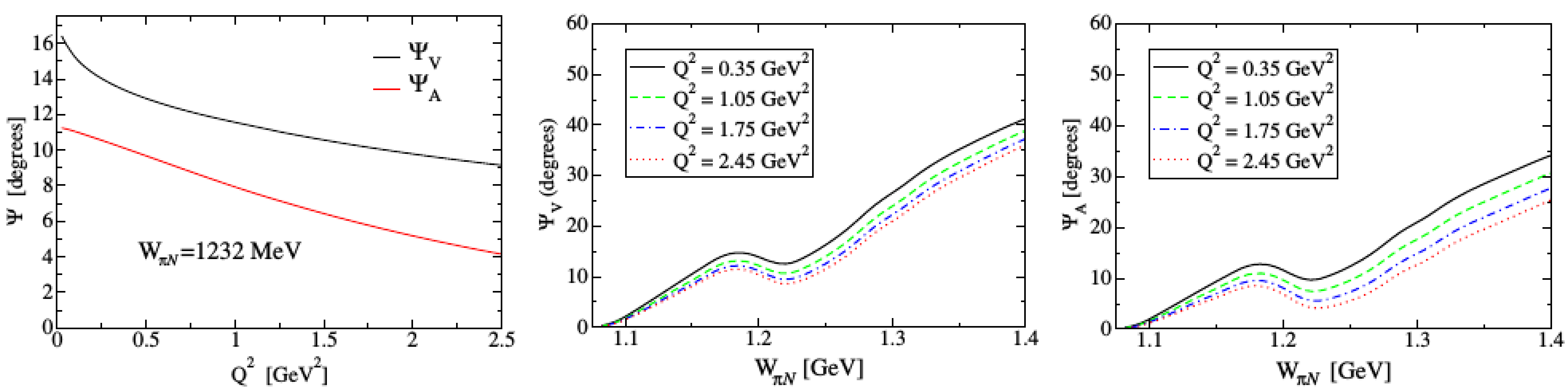

Pomeron

P. Allen et al. / Single meson production

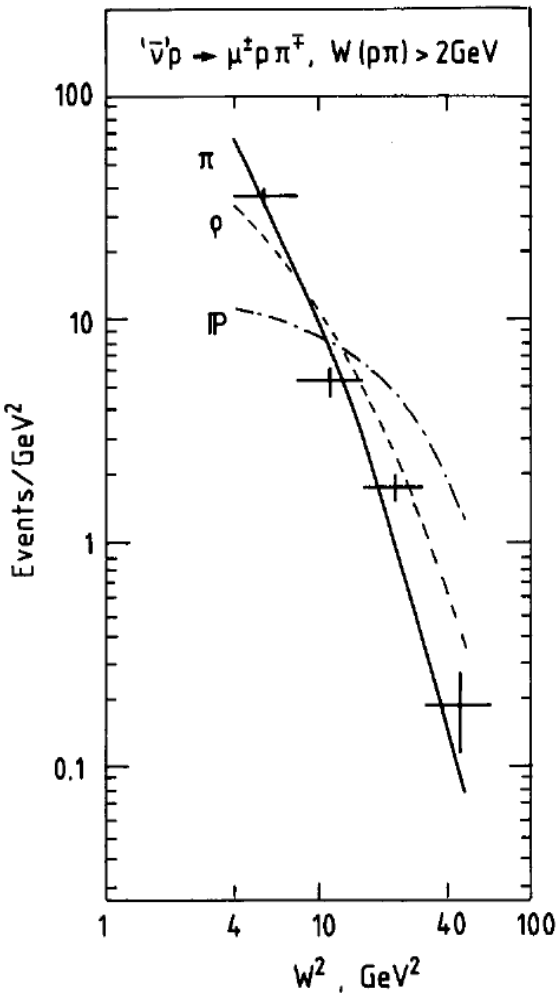

Nuclear Physics B264 (1986) 221–242

distribution is shown in fig. 11. The curves shown are normalised to the total number of events and correspond to pion exchange ($\alpha = 0$), vector meson exchange (ρ^0, ω^0; $\alpha_0 = 0.5$) and pomeron exchange ($\alpha_0 = 1$). The data clearly exclude pomeron exchange and are compatible with pure pion exchange; some contribution of vector meson exchange cannot be excluded, however.

Fig. 11. Distribution of W^2 for the combined samples of reactions (1) and (2) with $W > 2.0$ GeV, with no cuts on other variables. Curves are from a Regge model calculation described in the text.

Relativistic mean-field model (I)

RMF model provides a microscopic description of the ground state of finite nuclei which is consistent with Quantum Mechanic, Special Relativity and symmetries of strong interaction.

The starting point is a Lorentz covariant Lagrangian density

Extension of the original σ–ω Walecka model (Ann. Phys.83,491 (1974)).

$$
\begin{aligned}
\mathcal{L} &= \overline{\Psi}\left(i\gamma_\mu\partial^\mu - M\right)\Psi + \frac{1}{2}\left(\partial_\mu\sigma\partial^\mu\sigma - m_\sigma^2\sigma^2\right) - U(\sigma) \\
&- \frac{1}{4}\Omega_{\mu\nu}\Omega^{\mu\nu} + \frac{1}{2}m_\omega^2\omega_\mu\omega^\mu - \frac{1}{4}\mathbf{R}_{\mu\nu}\mathbf{R}^{\mu\nu} + \frac{1}{2}m_\rho^2\boldsymbol{\rho}_\mu\boldsymbol{\rho}^\mu - \frac{1}{4}F_{\mu\nu}F^{\mu\nu} \\
&- g_\sigma\overline{\Psi}\sigma\Psi - g_\omega\overline{\Psi}\gamma_\mu\omega^\mu\Psi - g_\rho\overline{\Psi}\gamma_\mu\boldsymbol{\tau}\boldsymbol{\rho}^\mu\Psi - g_e\frac{1+\tau_3}{2}\overline{\Psi}\gamma_\mu A^\mu\Psi\,.
\end{aligned}
$$

where

$$
\begin{aligned}
\Omega^{\mu\nu} &= \partial^\mu\omega^\nu - \partial^\nu\omega^\mu\,, \\
\boldsymbol{R}^{\mu\nu} &= \partial^\mu\boldsymbol{\rho}^\nu - \partial^\nu\boldsymbol{\rho}^\mu\,, \\
F^{\mu\nu} &= \partial^\mu A^\nu - \partial^\nu A^\mu\,. \\
U(\sigma) &= \tfrac{1}{3}g_2\sigma^3 + \tfrac{1}{4}g_3\sigma^4
\end{aligned}
$$

Main approximations:

1) Mean-field approximation:

$\omega_\mu \rightarrow \langle\omega_\mu\rangle$ $\quad \sigma \rightarrow \langle\sigma\rangle$ $\quad \boldsymbol{\rho}_\mu \rightarrow \langle\boldsymbol{\rho}_\mu\rangle$

2) Static limit:

$\partial^0\omega_0 = \partial^0\boldsymbol{\rho}_0 = \partial^0\sigma = 0$ $\quad \omega_\mu = \delta_{\mu 0}\omega_0\,, \quad \boldsymbol{\rho}_\mu = \delta_{\mu 0}\boldsymbol{\rho}_0$

3) Spherical symmetry for finite nuclei:

$\omega_0 = \omega_0(r)$ $\quad \boldsymbol{\rho}_0 = \boldsymbol{\rho}_0(r)$ $\quad \sigma = \sigma(r)$

Relativistic mean-field model (II)

Dirac equation for nucleons (eq. of motion for the barionic fields):

$$[-i\boldsymbol{\alpha}\cdot\boldsymbol{\nabla} + V(r) + \beta(M + S(r))]\Psi_i(\boldsymbol{r}) = E_i\Psi_i(\boldsymbol{r})$$

where the scalar (S) and vector (V) potential are given by:

$$\begin{aligned} S(r) &= g_\sigma \sigma(r)\,, \\ V(r) &= g_\omega \omega^0(r) + g_\rho \tau_3 \rho_3^0(r) + e\frac{1+\tau_3}{2}A^0(r) \end{aligned}$$

Eqs. of motion for the mesons and the photon:

$$\begin{aligned} \left[-\nabla^2 + m_\sigma^2\right]\sigma(r) &= -g_\sigma \rho_s(r) - g_2\sigma^2(r) - g_3\sigma^3(r)\,, \\ \left[-\nabla^2 + m_\omega^2\right]\omega^0(r) &= -g_\omega \rho_B(r)\,, \\ \left[-\nabla^2 + m_\rho^2\right]\rho_3^0(r) &= -g_\rho \rho_\rho(r)\,, \\ -\nabla^2 A^0 &= e\rho_c\,, \end{aligned}$$

Current densities

$$\begin{aligned} \rho_s(r) &= \sum_i^A \overline{\Psi}_i(\boldsymbol{r})\Psi_i(\boldsymbol{r})\,, \\ \rho_B(r) &= \sum_i^A \Psi_i^\dagger(\boldsymbol{r})\Psi_i(\boldsymbol{r})\,, \\ \rho_\rho(r) &= \sum_i^A \Psi_i^\dagger(\boldsymbol{r})\tau_3\Psi_i(\boldsymbol{r}) \\ \rho_c(r) &= \sum_i^A \Psi_i^\dagger(\boldsymbol{r})\frac{1+\tau_3}{2}\Psi_i(\boldsymbol{r}) \end{aligned}$$

Solution of the couple equations for the fields in a self-consistent way.

Relativistic mean-field model (III)

In general, the parameters are fit to reproduce some general properties of some closed shell spherical nuclei and nuclear matter.

Parameters for the NLSH model (fitted to the mean charge radius, binding energy and neutron radius of the **^{16}O, ^{40}Ca, ^{90}Zr, ^{116}Sr, ^{124}Sn** and **^{208}Pb.**

M_N	m_σ	m_ω	m_ρ	g_σ	g_ω	g_ρ	g_2	g_3
939.0	526.059	783.0	763.0	10.444	12.945	4.3830	-6.9099	-15.8337

6 free parameters

$$[-i\boldsymbol{\alpha}\cdot\boldsymbol{\nabla} + V(r) + \beta(M + S(r)]\Psi_i(\boldsymbol{r}) = E_i\Psi_i(\boldsymbol{r})$$

$$\Psi_k^{m_j}(\boldsymbol{r}) = \begin{pmatrix} g_k(r)\varphi_k^{m_j}(\Omega_r) \\ i f_k(r)\varphi_{-k}^{m_j}(\Omega_r) \end{pmatrix},$$

$$\varphi_k^{m_j}(\Omega_r) = \sum_{m_\ell s}\langle \ell m_\ell \frac{1}{2} s | j m_j\rangle Y_\ell^{m_\ell}(\Omega_r)\chi^s$$

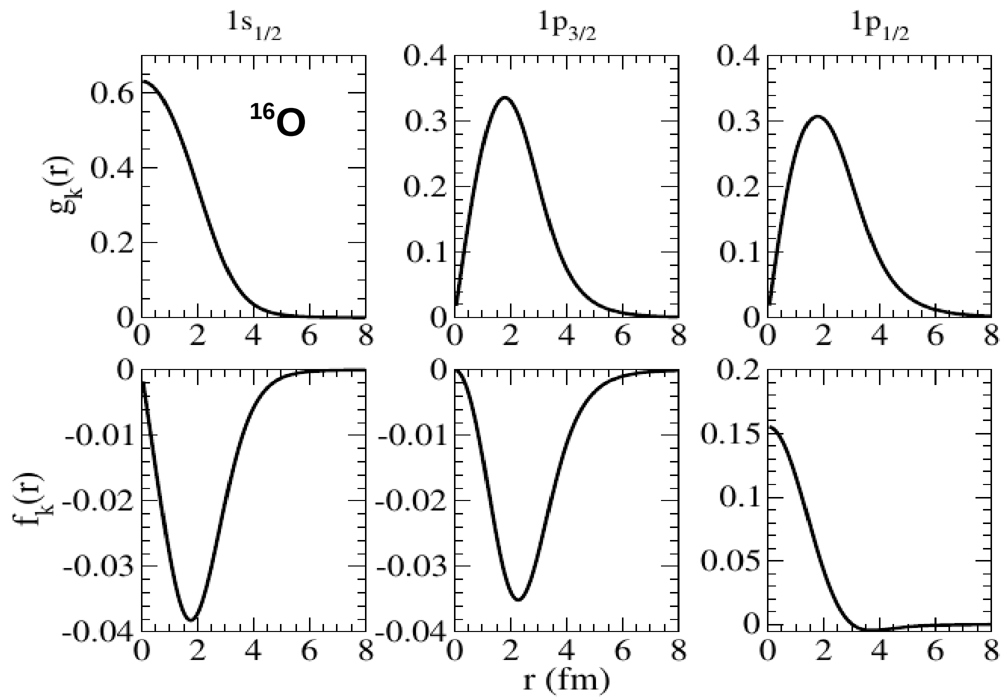

Relativistic mean-field model (IV)

J.A. Caballero et al. / Nuclear Physics A 632 (1998) 323–362 333

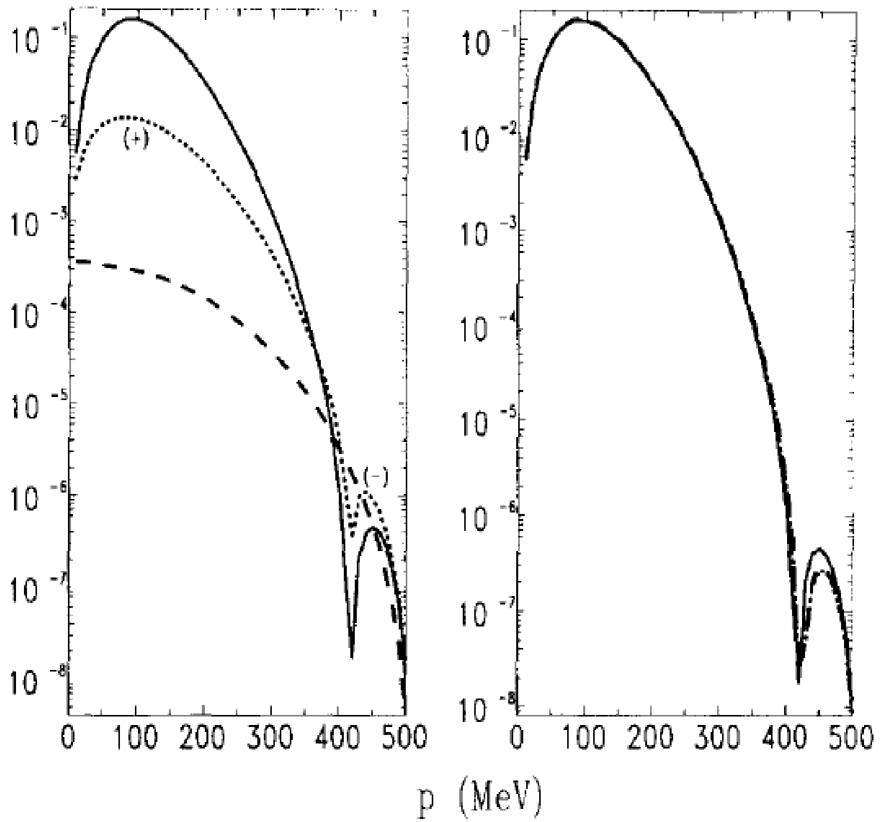

shell $1p_{1/2}$ in ^{16}O.

Fig. 1. Left panel: projection components of the momentum distribution (in units of fm^3): $N_{uu}(p)$ (solid), $N_{uv}(p)$ (dotted) and $N_{vv}(p)$ (dashed). Right panel: $N_{uu}(p)$ (solid), $N_{uu}^{(0)}(p)$ (dotted) and $N_{uu}^{n.r.}(p)$ (dashed) (see text for details).

RMF: quasielastic results

$$[-i\boldsymbol{\alpha}\cdot\boldsymbol{\nabla} + V(r) + \beta(M + S(r)]\Psi_i(\boldsymbol{r}) = E_i\Psi_i(\boldsymbol{r})$$

$$J^{\mu}_{had} = \sum_{i}^{A} \int d\mathbf{r}\, \overline{\Psi}_F(\mathbf{r})\, \hat{\mathcal{O}}^{\mu}_{one\text{-}body}\, \Psi_B(\mathbf{r})\, e^{i\mathbf{q}\cdot\mathbf{r}}$$

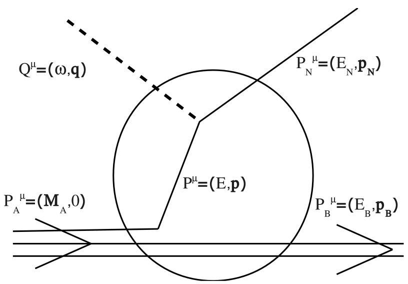

RPWIA: Scattered nucleon wf is described as a Dirac plane wave.

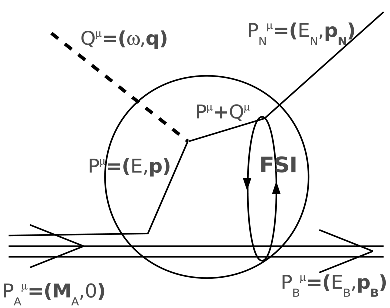

RMF-FSI: Scattered nucleon wf is solution of Dirac eq. in presence of the same potentials used to describe the bound nucleon wf.

Intermediate energies (typical QE regime)

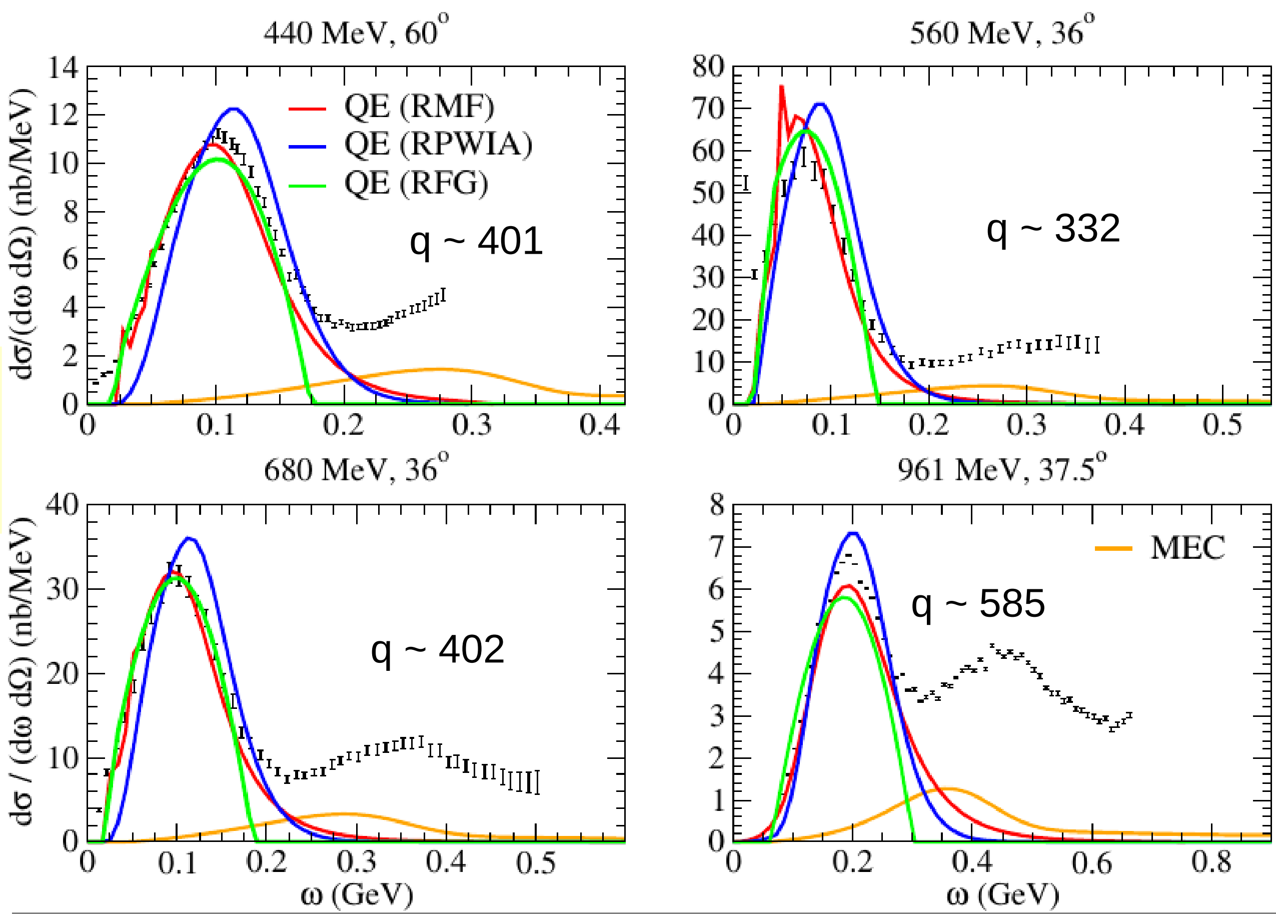

RMF: quasielastic results

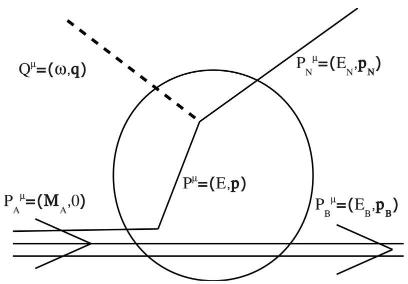

RPWIA: Scattered nucleon wf is described as a Dirac plane wave.

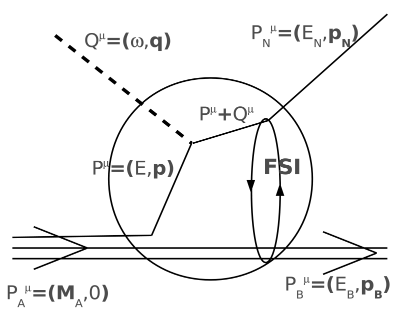

RMF-FSI: Scattered nucleon wf is solution of Dirac eq. in presence of the same potentials used to describe the bound nucleon wf.

$$[-i\boldsymbol{\alpha}\cdot\boldsymbol{\nabla}+V(r)+\beta(M+S(r)]\Psi_i(\boldsymbol{r})=E_i\Psi_i(\boldsymbol{r})$$

$$J^{\mu}_{had}=\sum_i^A\int d\mathbf{r}\,\overline{\Psi}_F(\mathbf{r})\,\hat{\mathcal{O}}^{\mu}_{one\text{-}body}\,\Psi_B(\mathbf{r})\,e^{i\mathbf{q}\cdot\mathbf{r}}$$

Low energies

High energies